Journal of Power Sources 226 (2013) 186–190

Contents lists available at SciVerse ScienceDirect

Journal of Power Sources

journal homepage: www.elsevier.com/locate/jpowsour

Short communication

Lattice orientation control of lithium cobalt oxide cathode film for all-solid-state thin film batteries

Yongsub Yoon, Chanhwi Park, Junghoon Kim, Dongwook Shin*

Division of Materials Science & Engineering, Hanyang University, 222 Wangwimni-ro, Seongdong-gu, Seoul 133-791, Republic of Korea

HIGHLIGHTS

- ► Lithium cobalt oxide thin film cathodes for the all-solid-state thin film batteries.
- ► The enhancement of ionic and electrical conductivities by controlling the lattice orientation.
- ► The improved rate performance of the cathode films with the controlled grain growth.

ARTICLE INFO

Article history:
Received 5 July 2012
Received in revised form
25 September 2012
Accepted 12 October 2012
Available online 7 November 2012

Keywords:
Lithium cobalt oxide
Lattice orientation control
Thin film batteries
Radio-frequency magnetron sputtering
Lithium-ion diffusivity

ABSTRACT

For the application to all-solid-state thin film batteries, $LiCoO_2$ thin films are deposited by RF-sputtering with controlling the lattice orientations to maximize lithium-ion diffusivity in film textures. The nano-sized crystalline grains grow up with the (003) preferred orientation parallel to the substrates at room temperature due to the lowest surface energy of this atomic plane. However, because the surface energy difference of atomic planes of $LiCoO_2$ reduces with increasing substrate temperature, the influence of surface energy becomes weaker at high temperature. The $LiCoO_2$ thin films with the (110) preferred orientation are obtained at higher temperatures by dominant influence from the lowest the volume strain energy of this orientation. To take advance of this orientation effect in full cell, the influences of the metallic current collector layer on the structural properties of sputtered cathode are investigated. It turns out that the Li_2O buffer layers between the cathode films and the metallic current collector layers can suppress the formation of lithium-deficient phase, Co_3O_4, and the growth of (003) plane by reducing the lattice match between of $LiCoO_2$ plane and Al(111) plane. The $LiCoO_2$ films with the controlled orientation show enhanced rate performance owing to improved interfacial resistance and lithium-ion conductivity.

1. Introduction

Needs for miniaturized electronic device have created demands on the development of all-solid-state thin film batteries [1,2]. This type of battery is suitable as a power source in medical diagnosis devices, drug delivery devices, active RF cards, miniature transmitters, personal data assistant systems and micro electro mechanical systems (MEMS) devices [3–5]. The micro battery cell is usually less than 10 μm in total thickness and aims for integration with microelectronic devices. Since the first epoch-making report on practical thin film battery was announced in 1982 from Hitachi Corporation, intensive efforts have been made to obtain high performance electrode and electrolyte materials for thin film batteries [6]. However, in spite of numerous research efforts, the real challenge still resides in finding appropriate thin film materials to satisfy the requirements imposed by of the electronic devices in terms of specific capacity, cycle life, reliability, and safety.

A lithium-ion battery contains an electrolyte, an anode, and a cathode. Electrolyte provides the separation of ionic transport and electronic transport, and electrodes act as a source or a reservoir of lithium ions. The electrode carries out the reversible electrochemical lithium insertion–extraction reaction during battery cycling. Thus, cathode system must provide the mobility of both lithium ions and electrons. However, many electrochemically active materials do not provide enough electronic conduction, so it is necessary to add supplementary electronic conducting materials such as carbon black. For example, olivine-type structure materials of $LiMPO_4$ ($M = 3^+$ cation) have intrinsic disadvantages such as low electronic conductivity lower than 10^{-9} S cm^{-1} and the low lithium-ion diffusivity preventing the realization of its theoretical

* Corresponding author. Tel.: +82 2 2220 0503; fax: +82 2 2220 4011.
E-mail address: dwshin@hanyang.ac.kr (D. Shin).

0378-7753/$ – see front matter © 2012 Elsevier B.V. All rights reserved.
http://dx.doi.org/10.1016/j.jpowsour.2012.10.094

capacity [7,8]. These drawbacks prevent it from being applied as a thin film cathode for all-solid-state thin film batteries since thin film cathode cannot contain additives such as conductive agents or binders. The electrochemical performance of cathode films should be maximized by fully utilizing their intrinsic properties.

Therefore, it is a natural consequence that $LiCoO_2$ thin films have received considerable attention as a cathode for thin film batteries due to their high electronic conductivity [9]. $LiCoO_2$ has hexagonal layered crystal structure, consisting of the rhombohedron constructed by cobalt and lithium alternately occupying octahedral sites between adjacent close-packed planes of oxygen [10–12]. It exhibits alternating Co^{3+} and Li^{+} planes in ABCABC stacking arrangement, with lithium ions in octahedral sites between O–Co–O sheets. Lithium-ion diffusion occurs via vacancy hopping mechanism within the lithium plane. Electrical properties of this layered structure will be strongly dependent on the crystal orientation due to its anisotropic crystal structure. Thus, in case of layered $LiCoO_2$ in all-solid-state thin film batteries, lithium-ion mobility and electrochemical reaction with the solid electrolyte and the current collector can be improved by minimizing the interfacial resistance of cathode layers through controlling growth orientation. Bouwman et al. [13] reported that the vertical alignment of (110) plane to the substrates is favorable for fast lithium-ion diffusion in the structures, while the lithium diffusivity of the thin films with (003) plane aligned horizontally to substrate is lower by a few orders of magnitude. Also, Dudney and Jang [14] reported the influence of cathode film thickness on the discharge properties of the thin film batteries. The crystallographic planes with (003) preferred orientation was grown horizontally to the substrate in the early stage of growth, while the grains with (101) and (104) planes parallel to the substrate were grown in the later stage for the films thicker than about ~1 μm.

However, in either study, homogeneous and stable microstructures with the desirable crystallographic orientation have not been achieved. Therefore, we investigated the method to control the lattice orientation of $LiCoO_2$ films to improve intercalation characteristics of all-solid-state battery. The structural alteration by various growth conditions was also investigated, and the effects of this microstructure control on electrochemical performance were studied.

2. Experimental

The lithium cobalt oxide thin films were deposited onto silicon substrates by radio-frequency magnetron sputtering. Silicon substrates were washed by HF, ethanol, and distilled water and dried thoroughly. A 2-inch commercial target (LTS, USA) was used, and it was bonded onto copper plates. $LiCoO_2$ sputtering was carried out under working pressure of 5×10^{-3} Torr with 90% Argon (5 N pure) – 10% oxygen (5 N pure) mixed gas. The RF power used for cathode deposition was 150 W, and the distance between the substrate and the target was 10 cm. The substrate holder was rotated to obtain homogeneous films. $LiCoO_2$ thin films show deposition rate of about 5–6.7 nm min^{-1}, and the thickness of the samples deposited for 60 min was about 300–400 nm. The targets were pre-sputtered for 30 min under the same conditions in order to eliminate impurities. The as-deposited $LiCoO_2$ thin films were annealed at 500 °C for 2 h in air.

For the investigation of the metallic current collector effect, the aluminum metal was sputtered with thickness of ~20 nm on silicon wafers. Also, Li_2O/Al/Si substrates were prepared by depositing Li_2O for 10 min on the Al current collector film to control the influence of the metallic layer. The crystallographic orientation of cathode thin films was characterized by X-ray diffraction using a Rigaku Ultima IV with Cu-Kα radiation. The surface and cross-sectional morphology of thin films were observed by scanning electron microscopy (Hitachi S-4800, Japan). Electron-transparent samples for transmission electron microscopy investigations were prepared by using the combination of Focused Ion Beam (FIB) and scanning electron microscopy system (SMI-8300, Japan).

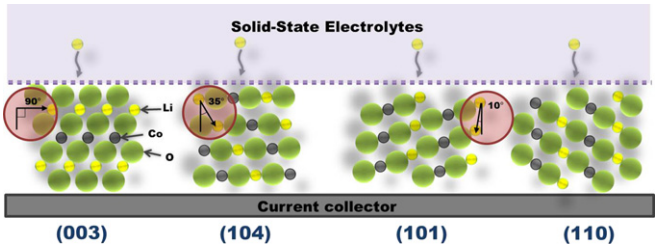

Fig. 1. Lithium-ion diffusion and intercalation pathway in $LiCoO_2$ thin film layers oriented to various lattice planes.

To evaluate the electrochemical properties, the 2032 coin-type half-cells were used. The cells were made up of lithium foils as a counter and reference electrode, a $LiCoO_2$ cathode thin films deposited with an active area of ~1 cm^2 and a thickness of ~500 nm as a working electrode, and 1 M $LiPF_6$ in ethylene carbonate/diethyl carbonate (EC/DEC, 1:1 vol%) as electrolyte. The cells were electrochemically cycled over the voltage range of 3.3 and 4.1 V by applying the various current densities of 20–640 μA cm^{-2} at room temperature.

3. Results and discussion

Fig. 1 illustrates the intercalation pathways of lithium ions through various lattice planes of $LiCoO_2$ layers. The intercalation pathway for (003) plane is horizontal to substrate surface, while that of (110) plane is almost vertical to substrate surface. The angle between lithium-ion pathway and lattice planes is decreased from (003) to (110) plane. It is expected that $LiCoO_2$ films with different orientations should exhibit different diffusion kinetics. Takahashi et al. [15,16] demonstrated that the electrical resistance of (110) plane of $LiCoO_2$ structure is about two-orders of magnitude smaller than (003) plane. Generally, in the deposition of the anisotropic structures, the formation of the specific lattice plane can be explained by the minimization of the structural energy at a given condition. Bates et al. [17] have shown that the crystalline lattice

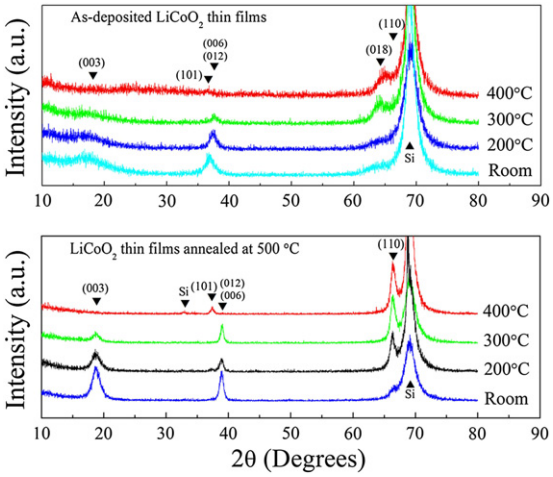

Fig. 2. X-ray diffraction patterns of the as-deposited and annealed lithium cobalt oxide thin films deposited at various substrate temperatures.

growth of $LiCoO_2$ thin films was determined by the competition between the surface energy and volume strain energy. In sputtered films thinner than ~1 μm, the most close-packed (003) plane evolves due to the domination surface energy, while for films thicker than 1 μm (110) plane grows by the dominating volume strain energy. Bouwman et al. reported the change in the preferred orientation in various deposition methods such as RF-sputtering and PLD using $LiCoO_2$ targets [12,13]. RF-sputtering and PLD films exhibit the preferred growth in (110) and (003), respectively. However, RF-sputtered films have also produced the film with (003) plane by prolonged sintering at high temperature.

Judged from these reports, to control the lattice growth direction in $LiCoO_2$ thin films, it is needed to control the balance between the surface energy and the volume strain energy of deposited layer. This was done by controlling growth temperature in this work. Fig. 2 shows the crystallographic evolution of $LiCoO_2$ thin films deposited at various temperatures. As-deposited film prepared at room temperature, similar to the precedent studies [12–14], exhibits broad diffraction peaks which correspond to close-packed planes such as (003) and (012) to minimize the surface energy. However, the intensities of (003) and (012) peaks were reduced by increasing the deposition temperature, while (018) and (110) peaks become more evident at the temperatures higher than 300 °C. It seems that, at high substrate temperature, the growth of film is mainly controlled by the volume strain energy effect. For the temperature dependence of the surface energy of an atomic plane in anisotropic lattice, it is possible to apply the well-known expression [18]:

$$\gamma T(hkl) = \gamma_0(hkl) + T\,\mathrm{d}\gamma(hkl)/\mathrm{d}T \quad (1)$$

where $\gamma_0(hkl)$ is the surface energy of a specific atomic plane at absolute zero, which is the intercept with y axis in the surface energy–temperature graph. In case of high surface energy planes, which has an atomically rough surface and the high surface entropy, should decrease more rapidly with increasing temperature [19,20]. As a result of this tendency, for the atomic plane with higher surface energy, the slope of the equation, $\mathrm{d}\gamma(hkl)/\mathrm{d}T$, becomes more negative. This means that the surface energy difference between various planes of anisotropic lattice will be reduced at high temperature.

Table 1
Surface energy [18] and volume strain energy [19] for several crystal planes (*hkl*) of $LiCoO_2$.

	Surface energy [J m^{-2}]	Volume strain energy [J m^{-3}]
(003)	0.4–1[a]	126.2
(014)	1.05	78.4
(110)	2.24	76.1

[a] The surface energy of lithium-terminated plane can vary from about 0.4 J m^{-2} at low lithium chemical potentials to about 1 J m^{-2} at high potentials.

Table 1 shows the surface energy [21] and the volume strain energy [22] for lattice planes of $LiCoO_2$. The surface energy of $LiCoO_2$ can be obtained by first principle calculations based on Density Functional Theory (DFT). The volume stain energies for various $LiCoO_2$ lattice planes were calculated for alumina substrate [22]. Although Hart et al. reported these values for alumina substrate, the qualitative dependency of the volume strain energies on the lattice plane orientation of $LiCoO_2$ is expected to be similar regardless of substrate material. The surface energy of (003) plane, less than 1 J m^{-2}, is the lowest and the (110) plane has the largest surface energy, 2.24 J m^{-2}. It may be expected that, the surface energy of the (110) plane decreases more rapidly than that of the (003) plane as temperature rises. Hence, the anisotropy of the surface energy diminishes with increasing temperature, and the volume strain energy effect works as a major factor in $LiCoO_2$ film deposition. It can be seen from Table 1 that the volume strain energy of the (110) plane is only about half of that of (003) plane.

After annealing at 500 °C, all XRD patterns showed the increased crystallinity, and the peaks for the planes with high surface energy, such as (101) and (110), appeared in the patterns of the films deposited at elevated temperature. The surface and cross-sectional images of the $LiCoO_2$ thin films deposited on silicon substrates at various temperatures and annealed at 500 °C for 2 h are shown in Fig. 3. In the surface image of the film deposited at room

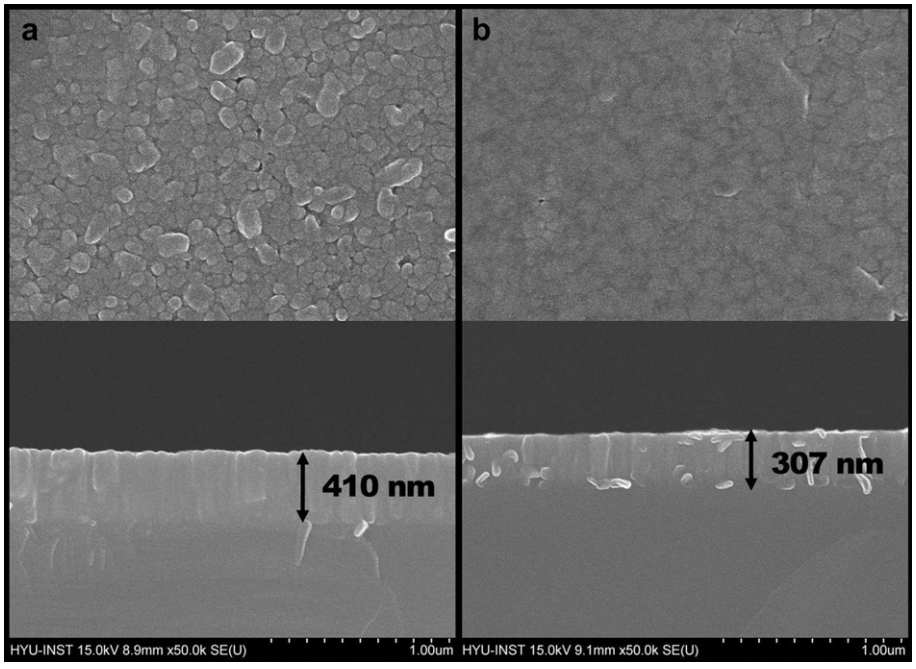

Fig. 3. Surface and cross-sectional images of the annealed lithium cobalt oxide deposited onto the silicon substrate temperatures of (a) room temperature and (b) 400 °C.

temperature, (a), the microstructure with rough morphology and low density is observed due to the grain growth vertical to the substrate, whereas the sample deposited at 400 °C, (b), showed uniform and dense surface. In cross-sectional images shown in the figures below, the thickness of $LiCoO_2$ film growth at 400 °C was thinner than room temperature sample. Due to the enhanced diffusion during the film growth, the film with higher density and smooth surface was obtained at higher temperature.

In all-solid-state thin film batteries, cathode layer is usually deposited on a metallic current collector layer rather than a bare substrate such as silicon or glass. This prompted the study on the influence of underlying metallic layers on the microstructural properties of $LiCoO_2$ film [14,23,24]. Bohne et al. [23] reported that strong preferred growth of (003) plane was detected for the metallic substrates such as platinum, stainless steel or titanium. Xia and Lu [24] explained that the lattice growth direction of $LiCoO_2$ on metallic current collectors depends on the atomic arrangement and the lattice parameter of metals. They reported that the (003) plane with the atomic spacing of ~2.81 Å grew easily on the Pt (111) film (2.77 Å) or the Au (111) film (2.88 Å). In our study, aluminum film with ~20 nm thickness was used as a current collector for measuring the electrochemical properties. Fig. 4(a) shows the X-ray diffraction spectra of $LiCoO_2$ thin films deposited at substrate temperature of 400 °C on Al/Si substrates. The $LiCoO_2$ films deposited on aluminum layer with lattice parameter of 2.86 Å (similar to Au (111); 2.88 Å) show four diffraction peaks of (003), (101), (006), and (104) planes [19]. Compared to the $LiCoO_2$ film sputtered on bare silicon shown in Fig. 2, the high substrate temperature seems to be less effective in reducing the preferred growth of (003) plane. Furthermore, the (311) main peak of Co_3O_4, Li-deficient structure produced by the Li–Al alloying reaction, was clearly observed (JCPDS No. 74-1657). Therefore, to compensate for the lithium-ion loss, Li_2O thin films were deposited at the interface between Al layer and $LiCoO_2$ film. Fig. 4(b) and (c) shows the XRD patterns of the $LiCoO_2$ films sputtered on the Li_2O/Al films at room temperature and 400 °C. One can see in the pattern (c) that the growth of (003) plane was completely suppressed while the growth of (110) plane ($2\theta = 66.3°$) was promoted. This improvement may be explained by the difference of the planar distance of the aluminum metal and Li_2O. The Li_2O (111) close-packed plane has a larger planar distance of about 3.26 Å than Al (111) of 2.86 Å. The (003) plane growth of $LiCoO_2$ film on Li_2O may be more difficult than on aluminum layers. The (110) plane growth in the pattern (c) may be explained by the reduced surface energy effect at elevated temperatures, which is similar explanation on the results in Fig. 2.

Fig. 5 shows the cross-sectional images of the $LiCoO_2$ thin films with the preferred orientation deposited on the Li_2O/Al/Si substrate at (a) room temperature and (b) 400 °C. The Li_2O layers are not clear in these figures due to thin thickness and the dissolution during annealing process. It can be seen that the (003) planes of $LiCoO_2$ grains are parallel to the substrate surface in Fig. 5(a), while (110) and (101) planes are vertically aligned to the substrate as shown in Fig. 5(b). The grain structures in $LiCoO_2$ films are well matched with XRD patterns shown in Fig. 4(b) and (c).

From the results, it is expected that these orientation-controlled $LiCoO_2$ thin films will show better electrochemical performance on battery cycling. Fig. 6 shows the charge–discharge curves of the half-cells of the $LiCoO_2$ thin film cathodes with (a) (003) and (b) (110) preferred orientation. The cell was charged and discharged between 3.3 and 4.1 V vs. Li at various current densities of 20–640 μA cm^{-2}. The polarization increases quickly and the specific capacity drops rapidly with increasing the current density for the (003)-oriented $LiCoO_2$ cathode. In contrast, the change in voltage profile and specific capacity of the (110)-oriented film are less significant. This result can be explained by the difference in the

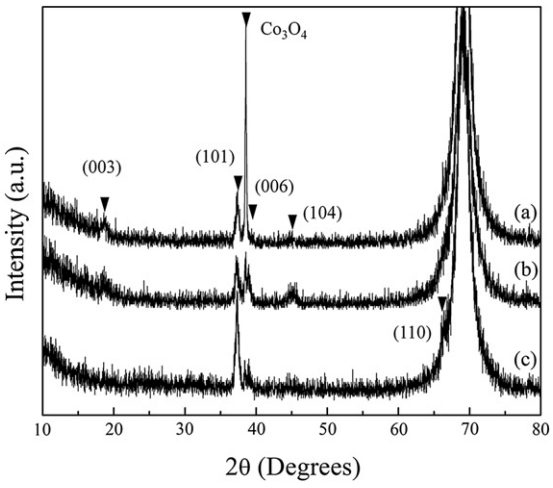

Fig. 4. X-ray diffraction patterns of lithium cobalt oxide thin films deposited (a) on the Al/Si substrate at 400 °C, and on the Li_2O/Al/Si substrate at (b) room temperature and (c) 400 °C. Thin films were annealed at 500 °C for 2 h.

interfacial resistances of (003) and (110) oriented films. The (110) oriented films with the high lithium-ion conductivity will show the lower polarizations during charge and discharge reactions because of the better cathode-electrolyte electrochemical intercalation

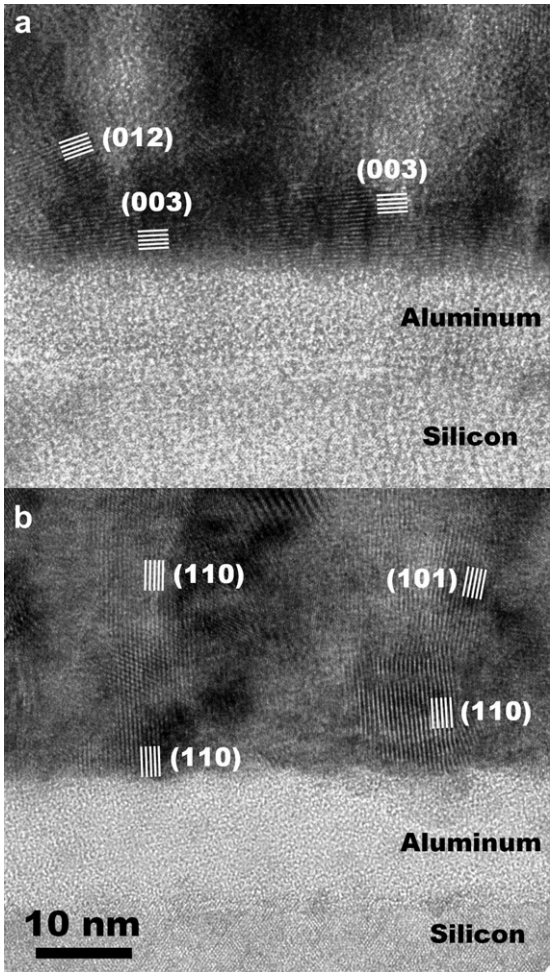

Fig. 5. The grain structures of lithium cobalt oxide films deposited on the Li_2O/Al/Si substrate at (a) room temperature and (b) 400 °C. The thin films were annealed at 500 °C for 2 h.

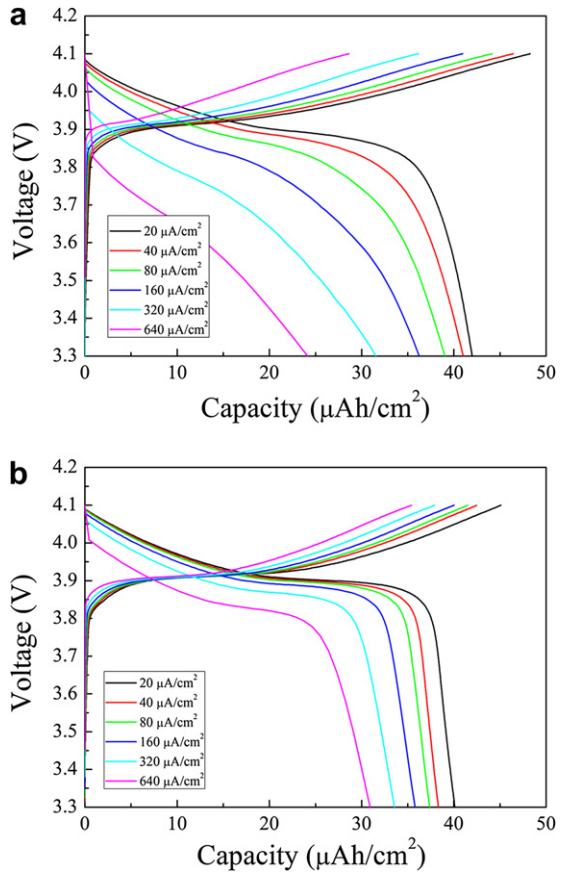

Fig. 6. Charge–discharge voltage profiles of coin-type half-cells with (a) (003) and (b) (110) oriented $LiCoO_2$ thin film cathodes at various current density of 20–640 μA cm^{-2}.

capability. The (110) oriented films exhibit the improved capacity retention as shown the rate performances in Fig. 7. For accurate comparison of the rate performance during discharging, the samples were charged at fixed rate of 20 μA cm^{-2}. Although the initial cycle discharge capacities of (003) and (110) oriented $LiCoO_2$ cathodes were similar, 42.4 and 40.6 μAh cm^{-2}, the lower ionic conducting (003) oriented cathode film showed dramatic capacity reduction as the discharge current density increased. At 640 μA cm^{-2}, each cathode films showed the discharge capacity of

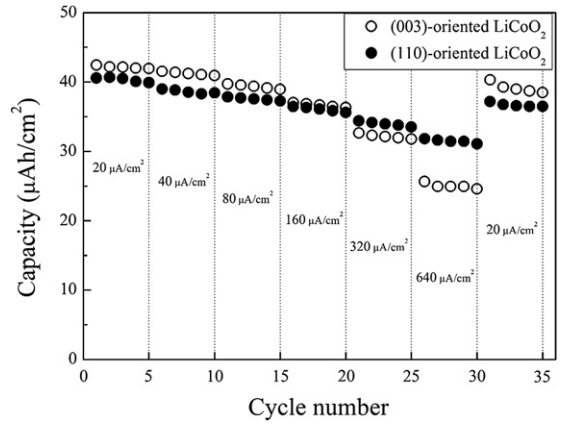

Fig. 7. Rate performances of coin-type half-cells with (003) and (110) oriented $LiCoO_2$ thin film cathodes at various current density of 20–640 μA cm^{-2}.

24.9 and 31.5 μAh cm^{-2} and the cycling efficiency of 58.7 and 77.6% of its initial capacity, respectively.

4. Conclusions

Achieving homogeneous and stable electrochemical properties of the $LiCoO_2$ thin film has remained elusive because no effective method to control the lattice orientation during the deposition was proposed. We investigated the preparation of nano-scale $LiCoO_2$ films with the controlled lattice orientations to obtain excellent intercalation characteristics in all-solid-state battery. $LiCoO_2$ grows up to the layered structures with the (003) plane parallel to the substrates at room temperature. However, as the substrate temperature rises, the surface energy difference of each atomic plane in the anisotropic structure reduces and, hence, the surface energy effect is diminished appreciably at 400 °C. Consequently, we obtained the $LiCoO_2$ thin films with the (110) or (101) preferred orientation since the volume strain energy effect is dominant at the elevated temperature. In addition, the Li_2O buffer layers between $LiCoO_2$ and metallic current collector films were able to control not only lithium loss but also the formation of desirable grain structure by the lattice mismatch of the Al (111) plane and the $LiCoO_2$ (003) plane. In the rate performances of coin-type half-cells, the cathode films with (110) preferred orientation showed much improved performance than the (003) films.

Acknowledgment

This research was supported by a grant from the Fundamental R&D Program for Core Technology of Materials funded by the Korean Ministry of Knowledge Economy (grant no. 10037233).

References

[1] J.N. Harb, R.M. Lafollette, R.H. Selfridge, L.L. Howelld, J. Power Sources 104 (2002) 46–51.
[2] F. Albano, M.D. Chung, D. Blaauw, D.M. Sylvester, K.D. Wise, A.M. Sastry, J. Power Sources 170 (2007) 216–224.
[3] A. Lavasseur, M. Menetrier, R. Dormoy, G. Meunier, Mater. Sci. Eng. B 3 (1989) 5–12.
[4] C.V. Ramana, K. Zahib, C.M. Julien, Chem. Mater. 18 (2006) 1397–1400.
[5] J.L. Souquet, M. Duclot, Solid State Ionics 148 (2002) 375–379.
[6] T. Minami, M. Tatsumisago, M. Wakihara, C. Iwakura, S. Kohjiya, I. Tanaka, Solid State Ionics for Batteries, Springer-Verlag, Tokyo, 2005.
[7] C. Yada, Y. Iriyama, S. Jeong, T. Abe, M. Inaba, Z. Ogumi, J. Power Sources 146 (2005) 559–564.
[8] Z. Li, D. Zhang, F. Yang, J. Mater. Sci. 44 (2009) 2435–2443.
[9] K. Mizushima, P.C. Jones, P.J. Wiseman, J.B. Goodenough, Mater. Res. Bull. 15 (1980) 783–789.
[10] J.D. Perkins, C.S. Bahn, J.M. McGraw, P.A. Parilla, D.S. Ginley, J. Electrochem. Soc. 148 (2001) A1302–A1312.
[11] S.B. Tang, L. Lu, M.O. Lai, Philos. Mag. 85 (2005) 2831–2842.
[12] P.J. Bouwman, B.A. Boukamp, H.J.M. Bouwmeester, H.J. Wondergem, P.H.L. Notten, J. Electrochem. Soc. 148 (2001) A311–A317.
[13] P.J. Bouwman, B.A. Boukamp, H.J.M. Bouwmeester, P.H.L. Notten, Solid State Ionics 152–153 (2002) 181–188.
[14] N.J. Dudney, Y.I. Jang, J. Power Sources 119–121 (2003) 300–304.
[15] Y. Takahashi, Y. Gotoh, J. Akimoto, S. Mizuta, K. Tokiwa, T. Watanabe, J. Solid State Chem. 164 (2002) 1–4.
[16] J. Xie, N. Imanishi, T. Matsumura, A. Hirano, Y. Takeda, O. Yamamoto, Solid State Ionics 179 (2008) 362–370.
[17] J.B. Bates, N.J. Dudney, B.J. Neudecker, F.X. Hart, H.P. Jun, S.A. Hackney, J. Electrochem. Soc. 147 (2000) 59–70.
[18] I.G. Shebzukhova, L.P. Aref'eva, K.B. Khokonov, Phys. Metals Metallogr. 105 (2008) 338–342.
[19] M. McLean, H. Mykura, Surf. Sci. 5 (1966) 466–481.
[20] B.E. Sundquist, Acta Met. 12 (1964) 585–592.
[21] D. Kramer, G. Ceder, Chem. Mater. 21 (2009) 3799–3809.
[22] F.X. Hart, J.B. Bates, J. Appl. Phys. 83 (1998) 7560–7566.
[23] L. Bohne, T. Pirk, W. Jaegermann, J. Solid State Electrochem., in press.
[24] H. Xia, L. Lu, Electrochim. Acta 52 (2007) 7014–7021.